



## Improved Measurements of Branching Fractions for $B \rightarrow K\pi, \pi\pi$ and $K\bar{K}$ Decays

Y. Chao,<sup>23</sup> K. Suzuki,<sup>7</sup> Y. Unno,<sup>2</sup> K. Abe,<sup>7</sup> K. Abe,<sup>39</sup> T. Abe,<sup>7</sup> I. Adachi,<sup>7</sup> H. Aihara,<sup>41</sup>  
M. Akatsu,<sup>20</sup> Y. Asano,<sup>46</sup> T. Aso,<sup>45</sup> V. Aulchenko,<sup>1</sup> T. Aushev,<sup>11</sup> A. M. Bakich,<sup>36</sup>  
S. Banerjee,<sup>37</sup> I. Bizjak,<sup>12</sup> A. Bondar,<sup>1</sup> A. Bozek,<sup>24</sup> M. Bračko,<sup>18,12</sup> T. E. Browder,<sup>6</sup>  
P. Chang,<sup>23</sup> B. G. Cheon,<sup>35</sup> R. Chistov,<sup>11</sup> S.-K. Choi,<sup>5</sup> Y. Choi,<sup>35</sup> Y. K. Choi,<sup>35</sup>  
A. Chuvikov,<sup>31</sup> S. Cole,<sup>36</sup> M. Danilov,<sup>11</sup> M. Dash,<sup>47</sup> L. Y. Dong,<sup>9</sup> J. Dragic,<sup>19</sup>  
A. Drutskoy,<sup>11</sup> S. Eidelman,<sup>1</sup> V. Eiges,<sup>11</sup> N. Gabyshev,<sup>7</sup> A. Garmash,<sup>31</sup> T. Gershon,<sup>7</sup>  
B. Golob,<sup>17,12</sup> A. Gordon,<sup>19</sup> J. Haba,<sup>7</sup> T. Hara,<sup>28</sup> M. Hazumi,<sup>7</sup> I. Higuchi,<sup>40</sup> T. Hokuue,<sup>20</sup>  
Y. Hoshi,<sup>39</sup> W.-S. Hou,<sup>23</sup> Y. B. Hsiung,<sup>23,\*</sup> H.-C. Huang,<sup>23</sup> T. Iijima,<sup>20</sup> K. Inami,<sup>20</sup>  
A. Ishikawa,<sup>7</sup> R. Itoh,<sup>7</sup> H. Iwasaki,<sup>7</sup> Y. Iwasaki,<sup>7</sup> J. H. Kang,<sup>49</sup> J. S. Kang,<sup>14</sup>  
P. Kapusta,<sup>24</sup> N. Katayama,<sup>7</sup> H. Kawai,<sup>2</sup> T. Kawasaki,<sup>26</sup> H. Kichimi,<sup>7</sup> H. J. Kim,<sup>49</sup>  
J. H. Kim,<sup>35</sup> K. Kinoshita,<sup>3</sup> S. Korpar,<sup>18,12</sup> P. Križan,<sup>17,12</sup> P. Krokovny,<sup>1</sup> A. Kuzmin,<sup>1</sup>  
Y.-J. Kwon,<sup>49</sup> J. S. Lange,<sup>4,32</sup> G. Leder,<sup>10</sup> S. H. Lee,<sup>34</sup> J. Li,<sup>33</sup> A. Limosani,<sup>19</sup>  
S.-W. Lin,<sup>23</sup> J. MacNaughton,<sup>10</sup> G. Majumder,<sup>37</sup> F. Mandl,<sup>10</sup> D. Marlow,<sup>31</sup>  
T. Matsumoto,<sup>43</sup> A. Matyja,<sup>24</sup> W. Mitaroff,<sup>10</sup> H. Miyake,<sup>28</sup> H. Miyata,<sup>26</sup> D. Mohapatra,<sup>47</sup>  
T. Mori,<sup>42</sup> T. Nagamine,<sup>40</sup> Y. Nagasaka,<sup>8</sup> T. Nakadaira,<sup>41</sup> E. Nakano,<sup>27</sup> M. Nakao,<sup>7</sup>  
H. Nakazawa,<sup>7</sup> Z. Natkaniec,<sup>24</sup> S. Nishida,<sup>7</sup> O. Nitoh,<sup>44</sup> S. Noguchi,<sup>21</sup> T. Nozaki,<sup>7</sup>  
S. Ogawa,<sup>38</sup> T. Ohshima,<sup>20</sup> S. Okuno,<sup>13</sup> S. L. Olsen,<sup>6</sup> W. Ostrowicz,<sup>24</sup> H. Ozaki,<sup>7</sup>  
P. Pakhlov,<sup>11</sup> H. Palka,<sup>24</sup> C. W. Park,<sup>14</sup> H. Park,<sup>15</sup> N. Parslow,<sup>36</sup> L. S. Peak,<sup>36</sup>  
L. E. Piilonen,<sup>47</sup> M. Rozanska,<sup>24</sup> H. Sagawa,<sup>7</sup> S. Saitoh,<sup>7</sup> Y. Sakai,<sup>7</sup> O. Schneider,<sup>16</sup>  
J. Schümann,<sup>23</sup> A. J. Schwartz,<sup>3</sup> S. Semenov,<sup>11</sup> M. E. Sevier,<sup>19</sup> H. Shibuya,<sup>38</sup>  
B. Shwartz,<sup>1</sup> V. Sidorov,<sup>1</sup> J. B. Singh,<sup>29</sup> N. Soni,<sup>29</sup> S. Stanič,<sup>46,†</sup> M. Starič,<sup>12</sup>  
K. Sumisawa,<sup>28</sup> T. Sumiyoshi,<sup>43</sup> S. Suzuki,<sup>48</sup> S. Y. Suzuki,<sup>7</sup> O. Tajima,<sup>40</sup> F. Takasaki,<sup>7</sup>  
N. Tamura,<sup>26</sup> M. Tanaka,<sup>7</sup> Y. Teramoto,<sup>27</sup> T. Tomura,<sup>41</sup> K. Trabelsi,<sup>6</sup> T. Tsuboyama,<sup>7</sup>  
T. Tsukamoto,<sup>7</sup> S. Uehara,<sup>7</sup> K. Ueno,<sup>23</sup> T. Uglov,<sup>11</sup> S. Uno,<sup>7</sup> G. Varner,<sup>6</sup> C. H. Wang,<sup>22</sup>  
J. G. Wang,<sup>47</sup> M.-Z. Wang,<sup>23</sup> M. Watanabe,<sup>26</sup> Y. Yamada,<sup>7</sup> A. Yamaguchi,<sup>40</sup>  
H. Yamamoto,<sup>40</sup> Y. Yamashita,<sup>25</sup> M. Yamauchi,<sup>7</sup> H. Yanai,<sup>26</sup> Heyoung Yang,<sup>34</sup> J. Ying,<sup>30</sup>  
Y. Yuan,<sup>9</sup> S. L. Zang,<sup>9</sup> J. Zhang,<sup>7</sup> Z. P. Zhang,<sup>33</sup> V. Zhilich,<sup>1</sup> and D. Žontar<sup>17,12</sup>

(The Belle Collaboration)

<sup>1</sup>*Budker Institute of Nuclear Physics, Novosibirsk*

<sup>2</sup>*Chiba University, Chiba*

<sup>3</sup>*University of Cincinnati, Cincinnati, Ohio 45221*

<sup>4</sup>*University of Frankfurt, Frankfurt*

<sup>5</sup>*Gyeongsang National University, Chinju*

<sup>6</sup>*University of Hawaii, Honolulu, Hawaii 96822*

- <sup>7</sup>*High Energy Accelerator Research Organization (KEK), Tsukuba*  
<sup>8</sup>*Hiroshima Institute of Technology, Hiroshima*  
<sup>9</sup>*Institute of High Energy Physics, Chinese Academy of Sciences, Beijing*  
<sup>10</sup>*Institute of High Energy Physics, Vienna*  
<sup>11</sup>*Institute for Theoretical and Experimental Physics, Moscow*  
<sup>12</sup>*J. Stefan Institute, Ljubljana*  
<sup>13</sup>*Kanagawa University, Yokohama*  
<sup>14</sup>*Korea University, Seoul*  
<sup>15</sup>*Kyungpook National University, Taegu*  
<sup>16</sup>*Swiss Federal Institute of Technology of Lausanne, EPFL, Lausanne*  
<sup>17</sup>*University of Ljubljana, Ljubljana*  
<sup>18</sup>*University of Maribor, Maribor*  
<sup>19</sup>*University of Melbourne, Victoria*  
<sup>20</sup>*Nagoya University, Nagoya*  
<sup>21</sup>*Nara Women's University, Nara*  
<sup>22</sup>*National Lien-Ho Institute of Technology, Miao Li*  
<sup>23</sup>*Department of Physics, National Taiwan University, Taipei*  
<sup>24</sup>*H. Niewodniczanski Institute of Nuclear Physics, Krakow*  
<sup>25</sup>*Nihon Dental College, Niigata*  
<sup>26</sup>*Niigata University, Niigata*  
<sup>27</sup>*Osaka City University, Osaka*  
<sup>28</sup>*Osaka University, Osaka*  
<sup>29</sup>*Panjab University, Chandigarh*  
<sup>30</sup>*Peking University, Beijing*  
<sup>31</sup>*Princeton University, Princeton, New Jersey 08545*  
<sup>32</sup>*RIKEN BNL Research Center, Upton, New York 11973*  
<sup>33</sup>*University of Science and Technology of China, Hefei*  
<sup>34</sup>*Seoul National University, Seoul*  
<sup>35</sup>*Sungkyunkwan University, Suwon*  
<sup>36</sup>*University of Sydney, Sydney NSW*  
<sup>37</sup>*Tata Institute of Fundamental Research, Bombay*  
<sup>38</sup>*Toho University, Funabashi*  
<sup>39</sup>*Tohoku Gakuin University, Tagajo*  
<sup>40</sup>*Tohoku University, Sendai*  
<sup>41</sup>*Department of Physics, University of Tokyo, Tokyo*  
<sup>42</sup>*Tokyo Institute of Technology, Tokyo*  
<sup>43</sup>*Tokyo Metropolitan University, Tokyo*  
<sup>44</sup>*Tokyo University of Agriculture and Technology, Tokyo*  
<sup>45</sup>*Toyama National College of Maritime Technology, Toyama*  
<sup>46</sup>*University of Tsukuba, Tsukuba*  
<sup>47</sup>*Virginia Polytechnic Institute and State University, Blacksburg, Virginia 24061*  
<sup>48</sup>*Yokkaichi University, Yokkaichi*  
<sup>49</sup>*Yonsei University, Seoul*

## Abstract

We report improved measurements of branching fractions for  $B \rightarrow K\pi$ ,  $\pi^+\pi^-$ ,  $\pi^+\pi^0$  and  $K\overline{K}$  decays based on a data sample of 85.0 million  $B\overline{B}$  pairs collected at the  $\Upsilon(4S)$  resonance with the Belle detector at the KEKB  $e^+e^-$  storage ring. This data sample is almost three times larger than the sample previously used. We observe clear signals for  $B \rightarrow K\pi$ ,  $\pi^+\pi^-$  and  $\pi^+\pi^0$  decays and set upper limits on  $B \rightarrow K\overline{K}$  decays. The results can be used to give model-dependent constraints on the CKM angle  $\phi_3$ , as well as limits on the hadronic uncertainty in the time-dependent analysis of the angle  $\phi_2$ .

PACS numbers: 11.30.Er, 12.15.Hh, 13.25.Hw, 14.40.Nd

---

\*on leave from Fermi National Accelerator Laboratory, Batavia, Illinois 60510

†on leave from Nova Gorica Polytechnic, Nova Gorica

Recent studies at  $B$  factories have significantly improved our knowledge of heavy-flavor physics. In particular, the establishment of mixing-induced  $CP$  violation in the  $B$ -meson system [1, 2] is encouraging for further tests of the Standard Model based on determinations of the Cabibbo-Kobayashi-Maskawa (CKM) matrix elements [3].

$B$ -meson decays to  $K\pi$ ,  $\pi\pi$  and  $K\bar{K}$  final states are dominated by  $b \rightarrow u$  tree and  $b \rightarrow s, d$  penguin diagrams. The properties of these decays provide information that can be used to determine the CKM angles  $\phi_2$  and  $\phi_3$  [4]. However, the extraction of these angles suffers from hadronic uncertainties present in the current theoretical description and from the small amplitudes of  $b \rightarrow u, s, d$  transitions. To solve these difficulties, various theoretical approaches based on flavor symmetries and dynamical calculations in the heavy-quark limit [5] have been proposed. In order to utilize these methods, the precision of the existing experimental results [6, 7, 8, 9, 10, 11, 12] must be improved.

In this paper, we report updated measurements of the branching fractions for  $B \rightarrow K\pi$ ,  $\pi^+\pi^-$ ,  $\pi^+\pi^0$  and  $K\bar{K}$  decays. Recent results for  $B^0 \rightarrow \pi^0\pi^0$  have been reported elsewhere [13, 14]. The measurements reported here are based on a  $78 \text{ fb}^{-1}$  data sample collected at the  $\Upsilon(4S)$  resonance, with the Belle detector [15] at the KEKB  $e^+e^-$  storage ring [16]. This sample corresponds to  $85.0 \pm 0.5$  million  $B\bar{B}$  pairs and is about three times larger than that used for our previous analysis [6]. The previous results are superseded with significantly improved statistical precision. Throughout this paper, neutral and charged  $B$  mesons are assumed to be produced in equal amounts at the  $\Upsilon(4S)$ . The inclusion of the charge conjugate decay is implied, unless explicitly stated.

The Belle detector is a large-solid-angle spectrometer consisting of a three-layer silicon vertex detector, a 50-layer central drift chamber (CDC), an array of threshold Cherenkov counters with silica aerogel radiators (ACC), time-of-flight scintillation counters, and an electromagnetic calorimeter comprised of CsI(Tl) crystals (ECL) located inside a superconducting solenoid coil that provides a 1.5 T magnetic field. An iron flux-return located outside of the coil is instrumented to detect  $K_L^0$  mesons and to identify muons. A detailed description of the Belle detector can be found elsewhere [15].

The basic analysis procedure is the same as described in Ref. [6]. However, the data sample used in this analysis was reprocessed with an improved tracking algorithm that reduces the probability of incorrectly associating CDC hits in the track finding. This improvement changes the efficiencies for the kinematic reconstruction of the signal as well as for the measurement of specific ionization energy loss ( $dE/dx$ ) in the CDC from the values given in Ref. [6].

The  $\pi^\pm$  mass is assigned to each charged track. Tracks used to form  $B$  candidates are required to originate from the interaction region based on their impact parameters.  $K_S^0$  mesons are reconstructed using pairs of oppositely charged tracks that have invariant masses in the range  $480 \text{ MeV}/c^2 < M_{\pi\pi} < 516 \text{ MeV}/c^2$ . A reconstructed  $K_S^0$  is required to have a displaced vertex and a flight direction consistent with that of a  $K_S^0$  originating from the interaction region. Pairs of photons with invariant masses in the range  $115 \text{ MeV}/c^2 < M_{\gamma\gamma} < 152 \text{ MeV}/c^2$  are used to form  $\pi^0$  mesons. The measured energy of each photon in the laboratory frame is required to be greater than 50 MeV in the barrel region, defined as  $32^\circ < \theta_\gamma < 128^\circ$ , and greater than 100 MeV in the end-cap regions, defined as  $17^\circ \leq \theta_\gamma \leq 32^\circ$  or  $128^\circ \leq \theta_\gamma \leq 150^\circ$ , where  $\theta_\gamma$  denotes the polar angle of the photon with respect to the  $e^-$  beam. Signal  $B$  candidates are required to satisfy  $5.27 \text{ GeV}/c^2 < M_{bc} < 5.29 \text{ GeV}/c^2$  and  $-0.3 \text{ GeV} < \Delta E < 0.5 \text{ GeV}$ , where  $M_{bc} = \sqrt{E_{\text{beam}}^{*2} - p_B^{*2}}$ ,  $\Delta E = E_B^* - E_{\text{beam}}^*$ ,  $E_{\text{beam}}^*$  is the beam-energy, and  $p_B^*$  and  $E_B^*$  are the momentum and energy of the reconstructed  $B$  meson,

all evaluated in the  $e^+e^-$  center-of-mass (CM) frame. The signal efficiencies of the kinematic reconstruction, estimated using GEANT-based [17] Monte Carlo (MC) simulations, are listed in Table I.

Charged tracks from  $B$  candidates have momenta ranging from 1.5 up to 4.5 GeV/ $c$  in the laboratory frame. They are distinguished as  $K^\pm$  or  $\pi^\pm$  mesons by the number of photoelectrons ( $N_{\text{p.e.}}$ ) detected by the ACC and  $dE/dx$  measured in the CDC. These quantities are used to form a  $K^\pm$  identification (KID) likelihood ratio  $\mathcal{R}_K = \mathcal{L}_K/(\mathcal{L}_K + \mathcal{L}_\pi)$ , where  $\mathcal{L}_K$  denotes the product of the individual likelihoods of  $N_{\text{p.e.}}$  and  $dE/dx$  for  $K^\pm$  mesons, and  $\mathcal{L}_\pi$  is the corresponding product for  $\pi^\pm$  mesons. The requirements on  $\mathcal{R}_K$  used in this analysis yield a  $K^\pm$  identification efficiency of 84.4% with a  $\pi^\pm$  misidentification rate of 5.3% for  $K^\pm$  candidates, and a  $\pi^\pm$  identification efficiency of 91.2% with a  $K^\pm$  misidentification rate of 10.2% for  $\pi^\pm$  candidates. The efficiencies and misidentification rates are measured by comparing the yields of high-momentum  $D^{*+}$ -tagged  $D^0 \rightarrow K^-\pi^+$  decays before and after applying the  $\mathcal{R}_K$  requirements. Here, the  $K^\pm$  and  $\pi^\pm$  momentum range is required to be the same as for the signal. Since the momentum and angular distributions are slightly different for  $D^0$  data and signal MC, the KID efficiencies are reweighted as a function of the polar angle of the signal track with respect to the  $e^-$  beam. In addition to the KID requirement, positively identified electrons are rejected using a similar likelihood ratio that also includes the energy deposited in the ECL.

The dominant background is due to the  $e^+e^- \rightarrow q\bar{q}$  ( $q = u, d, s, c$ ) continuum processes. A large MC sample shows that backgrounds from the  $b \rightarrow c$  transition are negligible since the momenta of their decay products are smaller than those in the signal decays. On the other hand, the momenta of the decay products from  $b \rightarrow u, s, d$  transitions other than the signal (denoted as other charmless  $B$  decays) can be as large as those in the signal decays. Events from these charmless  $B$  decays populate the negative  $\Delta E$  region because of the energy carried away by a photon or  $\pi$  meson, which is not used in the  $B$  reconstruction. We take these events into account in the signal extraction as discussed later.

We discriminate signal events from the  $q\bar{q}$  background by the event topology. This is quantified by the Super-Fox-Wolfram ( $SFW$ ) variable [6], which is a Fisher discriminant [18] formed from modified Fox-Wolfram moments [19]. The angle of the  $B$ -meson flight direction with respect to the beam axis in the CM frame ( $\theta_B$ ) provides additional discrimination. A signal likelihood ratio  $\mathcal{R}_s = \mathcal{L}_s/(\mathcal{L}_s + \mathcal{L}_{q\bar{q}})$  is used as the discriminating variable, where  $\mathcal{L}_s$  denotes the product of the individual  $SFW$  and  $\theta_B$  likelihoods for the signal, and  $\mathcal{L}_{q\bar{q}}$  is that for the  $q\bar{q}$  background. The probability density functions (PDFs) used for the likelihoods are derived from the MC for the signal, while events in the  $M_{\text{bc}}$  sideband ( $5.2 \text{ GeV}/c^2 < M_{\text{bc}} < 5.26 \text{ GeV}/c^2$  in the  $\Delta E$  acceptance) are used for the  $q\bar{q}$  background. We make a mode-dependent requirement on  $\mathcal{R}_s$  that maximizes  $N_s^{\text{exp}}/\sqrt{N_s^{\text{exp}} + N_{q\bar{q}}^{\text{exp}}}$ , where  $N_s^{\text{exp}}$  and  $N_{q\bar{q}}^{\text{exp}}$  denote the expected signal and  $q\bar{q}$  yields based on our previous measurements [6] (upper limits are used for  $K\bar{K}$  modes). The  $\mathcal{R}_s$  requirements eliminate more than 90% of the  $q\bar{q}$  background for the signal efficiencies given in Table I.

Signal yields are extracted using a binned maximum-likelihood fit to the  $\Delta E$  distributions after all the event selection requirements discussed above. The fitting function contains components for the signal,  $q\bar{q}$  background, and other charmless  $B$  decays. If applicable, possible reflections due to the  $K^\pm/\pi^\pm$  misidentification are included as additional components. All of the fit parameters other than the normalizations are fixed. The signal PDFs are based on the MC. For the modes with a  $\pi^0$  meson, the PDF is modeled with an empirically determined parametrization [20]. For the other modes, the sum of two Gaussian distributions

with a common mean is used for the PDF. Due to the  $\pi^\pm$  mass assumption, each  $K^\pm$  meson in the final state results in a shift in the peak position of about  $-45$  MeV. Discrepancies between the peak positions in data and MC are calibrated using  $B^+ \rightarrow \bar{D}^0 \pi^+$  decays, where the  $\bar{D}^0 \rightarrow K^+ \pi^- \pi^0$  sub-decay is used for the modes with  $\pi^0$  mesons and the  $\bar{D}^0 \rightarrow K^+ \pi^-$  sub-decay is used for the other modes. Here, the same analysis procedure used for the signal is applied except for the daughter particle reconstruction. The MC-based  $\Delta E$  resolutions are calibrated using invariant mass resolutions of high-momentum inclusive  $D$  decays. We use  $D^0 \rightarrow K^- \pi^+$  for the  $B^0 \rightarrow K^+ \pi^-$ ,  $\pi^+ \pi^-$ , and  $K^+ K^-$  modes,  $D^+ \rightarrow K_S^0 \pi^+$  for the  $B^+ \rightarrow K_S^0 \pi^+$ ,  $K_S^0 K^+$  and  $B^0 \rightarrow K_S^0 K_S^0$  modes, and  $D^0 \rightarrow K^- \pi^+ \pi^0$  for the modes with a  $\pi^0$  meson. The momentum ranges and reconstruction procedures for the  $D$  daughter particles are required to be the same as those for the signal daughter particles. The signal PDFs are also used for the reflections. The PDF of the  $q\bar{q}$  background is determined from the  $M_{bc}$  sideband data and modeled with a first-order polynomial for the  $K^+ K^-$  and  $K_S^0 K_S^0$  modes and a second-order polynomial for the other modes. The PDF for the other charmless  $B$  decays is taken from a smoothed histogram of a large MC sample. The  $K^+ \pi^0$  and  $\pi^+ \pi^0$  modes are fitted simultaneously with a fixed reflection-to-signal ratio that is determined from the measured KID efficiencies and misidentification rates. For other modes, all the normalizations are floated. All fit results are shown in Fig. 1.

The obtained signal yields are listed in Table II together with their statistical significances  $\mathcal{S} = \sqrt{-2 \ln(\mathcal{L}_0/\mathcal{L}_{N_s})}$ , where  $\mathcal{L}_0$  and  $\mathcal{L}_{N_s}$  denote the maximum likelihoods of the fits without and with the signal component, respectively. The fitted reflection yields are consistent within statistics with the expectations, which are derived from the fitted signal yields, KID efficiencies and misidentification rates, and the efficiencies of the  $R_s$  requirements. We observe clear signals for  $B \rightarrow K\pi$ ,  $\pi^+ \pi^-$  and  $\pi^+ \pi^0$  decays. For the decays  $B \rightarrow K\bar{K}$ , no significant signal is observed. We apply the Feldman-Cousins frequentist approach with systematic uncertainties taken into account [21] to obtain upper limits on the yields at the 90% confidence level (CL); these are used to set branching fraction upper limits. The branching fractions and upper limits are listed in Table II. Here, our latest measurement for  $B^0 \rightarrow \pi^0 \pi^0$  [13] based on a data sample of 152 million  $B\bar{B}$  pairs is also listed for completeness. The hierarchy of the branching fractions,  $\mathcal{B}(B \rightarrow K\pi) > \mathcal{B}(B \rightarrow \pi\pi)$ , is confirmed. More statistics are needed in order to firmly establish the position of  $B \rightarrow K\bar{K}$  in this hierarchy.

The systematic errors in the branching fractions are the quadratic sums of the systematic errors in the signal yields, uncertainties in the reconstruction efficiencies, and the 0.6% error in the number of  $B\bar{B}$  pairs. The systematic errors in the signal yields come from the uncertainties in the fit procedure. In order to study the sensitivity to the signal and  $q\bar{q}$  background PDFs, each shape parameter is independently varied by its error in the fit. The sensitivity to the contribution from other charmless  $B$  decays is evaluated by changing the minimum  $\Delta E$  requirement to  $-100$  MeV ( $-150$  MeV) for the modes without (with) a  $\pi^0$  meson, to exclude most of these events from the fit. The resulting changes in the signal yield are added in quadrature and assigned to the systematic errors on the signal yields as listed in Table II. The uncertainties in the reconstruction efficiencies are listed in Table III along with the test samples that are used. The uncertainty for the track finding efficiency in the high-momentum region is obtained by comparing the ratio of yields of fully reconstructed and partially reconstructed test samples in data and MC. The uncertainties in the  $K_S^0$  and  $\pi^0$  reconstruction efficiencies are obtained from similar comparisons of yield ratios in test samples. Here, the test samples are restricted to the same  $K_S^0$  and  $\pi^0$  momentum ranges as

the signal. The experimental errors in the branching fractions of these decays [22] are added in quadrature. The uncertainties in the KID efficiencies and misidentification rates are due to the statistics of the data test sample. We also checked the effect of the difference in the hadronic environment between the signal and test samples. No significant effect is seen in the efficiencies and misidentification rates. The  $\mathcal{R}_s$  requirement for each mode is applied to data and MC test samples, and the difference is included in the systematic error.

To a good approximation in the Standard Model, the relative weak phase between the penguin and tree amplitudes in  $K\pi$  modes is  $\phi_3$ . It is in principle possible to extract  $\phi_3$  if the hadronic uncertainties are under control. Several approaches to constrain  $\phi_3$  have been proposed using the ratios of partial widths for  $K\pi$  and  $\pi\pi$  modes with model-dependent assumptions on the hadronic uncertainties [5]; the ratios give cancellations of these uncertainties. We calculate such useful partial width ratios as listed in Table IV. Here, the ratio of charged to neutral  $B$  meson lifetimes  $\tau_{B^+}/\tau_{B^0} = 1.083 \pm 0.017$  [22] is used to convert the branching fraction ratios into partial width ratios if necessary, and the total errors are reduced because of the cancellation of the partially common systematic errors. Applying the approach of Buras and Fleischer [23], for illustration, our  $\Gamma(K^+\pi^-)/2\Gamma(K^0\pi^0)$  measurement excludes the region  $29^\circ < \phi_3 < 83^\circ$  at the 90% CL based on MC pseudo-experiments while that of  $2\Gamma(K^+\pi^0)/\Gamma(K^0\pi^+)$  gives no constraint. These results are obtained without any assumption on the tree-to-penguin amplitude ratio, but neglecting re-scattering effects and taking the size of the electroweak penguin as in Ref. [23]. Although a more aggressive constraint on  $\phi_3$  can be derived by introducing further model-dependent assumptions on the hadronic uncertainties, a coherent study of these approaches is required to reduce the model-dependence on hadronic uncertainties and to determine  $\phi_3$ .

A naive expectation for the tree-dominated  $\pi^+\pi^-$  and  $\pi^+\pi^0$  modes predicts  $2\Gamma(\pi^+\pi^0)/\Gamma(\pi^+\pi^-) = 1$ . The deviation of our result from this expectation, as given in Table IV, is consistent with our previous measurement [6] and would indicate the existence of a significant penguin contribution in the  $\pi^+\pi^-$  mode if the color-suppressed tree contribution plays a minor role [24]. This penguin contribution complicates the extraction of  $\phi_2$  from the time-dependent  $CP$  asymmetry in the  $\pi^+\pi^-$  mode (referred to as “penguin pollution”) [25]. Applying an approach based on the isospin relations in  $\pi\pi$  modes [26], our measured ratios  $\Gamma(\pi^+\pi^0)/\Gamma(\pi^+\pi^-)$  and  $\Gamma(\pi^0\pi^0)/\Gamma(\pi^+\pi^-)$  in Table IV give the 90% CL bound on the size of the “penguin pollution”  $|\theta| < 56^\circ$ ; the CL is derived from MC pseudo-experiments. Here, we also use the partial-rate  $CP$  asymmetry in the  $\pi^+\pi^-$  mode,  $\mathcal{A}_{\pi\pi} = +0.58 \pm 0.15 \pm 0.07$ , which is reported in Ref. [9].

In conclusion, we have measured or constrained the branching fractions for the  $B \rightarrow K\pi$ ,  $\pi^+\pi^-$ ,  $\pi^+\pi^0$  and  $K\bar{K}$  decays with 85.0 million  $B\bar{B}$  pairs collected on the  $\Upsilon(4S)$  resonance at the Belle experiment. We observe clear signals for  $B \rightarrow K\pi$ ,  $\pi^+\pi^-$  and  $\pi^+\pi^0$  decays and set upper limits on  $B \rightarrow K\bar{K}$  decays. The hierarchy of branching fractions reported in earlier measurements is confirmed. These results have significantly improved statistical precision compared to our previous measurements and supersede them. The results can be used to give model-dependent constraints on  $\phi_3$ , as well as limits on the hadronic uncertainty in the time-dependent analysis of  $\phi_2$ .

We wish to thank the KEKB accelerator group for the excellent operation of the KEKB accelerator. We acknowledge support from the Ministry of Education, Culture, Sports, Science, and Technology of Japan and the Japan Society for the Promotion of Science; the Australian Research Council and the Australian Department of Education, Science and Training; the National Science Foundation of China under contract No. 10175071; the De-

partment of Science and Technology of India; the BK21 program of the Ministry of Education of Korea and the CHEP SRC program of the Korea Science and Engineering Foundation; the Polish State Committee for Scientific Research under contract No. 2P03B 01324; the Ministry of Science and Technology of the Russian Federation; the Ministry of Education, Science and Sport of the Republic of Slovenia; the National Science Council and the Ministry of Education of Taiwan; and the U.S. Department of Energy.

- 
- [1] K. Abe *et al.* (Belle Collaboration), Phys. Rev. D **66**, 071102(R) (2002).
  - [2] B. Aubert *et al.* (BABAR Collaboration), Phys. Rev. Lett. **89**, 201802 (2002).
  - [3] N. Cabibbo, Phys. Rev. Lett. **10**, 531 (1963); M. Kobayashi and T. Maskawa, Prog. Theor. Phys. **49**, 652 (1973).
  - [4] See, for example, the review “ $CP$  Violation in  $B$  Decay — Standard Model Predictions” by H. Quinn and A. I. Sanda in Ref. [22]. ( $\alpha(=\phi_2)$  and  $\gamma(=\phi_3)$  are also used in the literature.)
  - [5] See, for example, the chapter “Future Directions” and its references, in “The CKM Matrix and the Unitarity Triangle”, M. Battaglia *et al.* (ed.), hep-ph/0304132 (2003).
  - [6] B. C. K. Casey *et al.* (Belle Collaboration), Phys. Rev. D **66**, 092002 (2002).
  - [7] Y. Unno *et al.* (Belle Collaboration), Phys. Rev. D **68**, 012001 (2003).
  - [8] K. Abe *et al.* (Belle Collaboration), Phys. Rev. D **68**, 012001 (2003).
  - [9] K. Abe *et al.* (Belle Collaboration), hep-ex/0401029 (2004).
  - [10] B. Aubert *et al.* (BABAR Collaboration), Phys. Rev. Lett. **87**, 151802 (2001); Phys. Rev. Lett. **91**, 021801 (2003).
  - [11] B. Aubert *et al.* (BABAR Collaboration), Phys. Rev. Lett. **89**, 281802 (2002).
  - [12] D. Cronin-Hennessy *et al.* (CLEO Collaboration), Phys. Rev. Lett. **85**, 515 (2000); S. Chen *et al.* (CLEO Collaboration), Phys. Rev. Lett. **85**, 525 (2000); D. M. Asner *et al.* (CLEO Collaboration), Phys. Rev. D **65**, 031103(R) (2002).
  - [13] S. H. Lee *et al.* (Belle Collaboration), Phys. Rev. Lett. **91**, 261801 (2003).
  - [14] B. Aubert *et al.* (BABAR Collaboration), Phys. Rev. Lett. **91**, 241801 (2003).
  - [15] A. Abashian *et al.* (Belle Collaboration), Nucl. Inst. Meth. A **479**, 117 (2002).
  - [16] S. Kurokawa and E. Kikutani *et al.*, Nucl. Inst. Meth. A **499**, 1 (2003) and other papers in this volume.
  - [17] R. Brun *et al.*, GEANT 3.21, CERN Report No. DD/EE/84-1 (1987).
  - [18] R. A. Fisher, Annals of Eugenics **7**, 179 (1936).
  - [19] G. C. Fox and S. Wolfram, Phys. Rev. Lett. **41**, 1581 (1978).
  - [20] J. E. Gaiser *et al.*, Phys. Rev. D **34**, 711 (1986).
  - [21] G. J. Feldman and R. D. Cousins, Phys. Rev. D **57**, 3873 (1998); J. Conrad *et al.*, Phys. Rev. D **67**, 012002 (2003).
  - [22] K. Hagiwara *et al.* (Particle Data Group), Phys. Rev. D **66**, 010001 (2002).
  - [23] A. J. Buras and R. Fleischer, Eur. Phys. J. C **16**, 97 (2000).
  - [24] M. Gronau and J. L. Rosner, Phys. Rev. D **65**, 013004 (2001).
  - [25] M. Gronau and D. London, Phys. Rev. Lett. **65**, 3381 (1990).
  - [26] M. Gronau *et al.*, Phys. Lett. B **514**, 315 (2001).



TABLE I: Signal efficiencies for kinematic reconstruction (Rec),  $\mathcal{R}_K$  requirements and  $\mathcal{R}_s$  requirement along with the sub-decay branching fraction ( $\mathcal{B}_{\text{sub}}$ ) for  $K^0 \rightarrow K_S^0 \rightarrow \pi^+\pi^-$  and total signal efficiencies.

Mode	Rec	$\mathcal{R}_K$	$\mathcal{R}_s$	$\mathcal{B}_{\text{sub}}$	Total
$K^+\pi^-$	0.731	0.769	0.672	—	0.378
$K^+\pi^0$	0.461	0.844	0.501	—	0.195
$K^0\pi^+$	0.571	0.911	0.560	0.343	0.100
$K^0\pi^0$	0.314	—	0.673	0.343	0.073
$\pi^+\pi^-$	0.756	0.830	0.560	—	0.352
$\pi^+\pi^0$	0.476	0.911	0.395	—	0.172
$K^+K^-$	0.727	0.713	0.387	—	0.201
$K^+\bar{K}^0$	0.539	0.844	0.388	0.343	0.061
$K^0\bar{K}^0$	0.447	—	0.561	0.235	0.059

TABLE II: Signal yields ( $N_s$ ), statistical significance ( $\mathcal{S}$ ), and branching fractions ( $\mathcal{B}$ ) for the  $B \rightarrow K\pi$ ,  $\pi^+\pi^-$ ,  $\pi^+\pi^0$  and  $K\bar{K}$  decays. The first and second errors are the statistical and systematic errors, respectively. For completeness, the  $\pi^0\pi^0$  results from Ref. [13] are also listed.

Mode	$N_s$	$\mathcal{S} [\sigma]$	$\mathcal{B} [10^{-6}]$
$K^+\pi^-$	$595.9 \pm 33.2 \pm 7.8$	24.1	$18.5 \pm 1.0 \pm 0.7$
$K^+\pi^0$	$198.9 \pm 21.5 \pm 15.6$	10.8	$12.0 \pm 1.3 \pm 1.3$
$K^0\pi^+$	$187.0 \pm 16.3 \pm 1.5$	16.4	$22.0 \pm 1.9 \pm 1.1$
$K^0\pi^0$	$72.6 \pm 14.0 \pm 4.9$	5.8	$11.7 \pm 2.3 \pm 1.2$
$\pi^+\pi^-$	$132.7 \pm 18.9 \pm 2.7$	8.5	$4.4 \pm 0.6 \pm 0.3$
$\pi^+\pi^0$	$72.4 \pm 17.4 \pm 3.7$	4.5	$5.0 \pm 1.2 \pm 0.5$
$\pi^0\pi^0$	$25.6 \pm 9.3 \pm 1.6$	3.5	$1.7 \pm 0.6 \pm 0.2$
$K^+K^-$	$-1.0 \pm 6.6$	0.0	$< 0.7$
$K^+\bar{K}^0$	$8.6 \pm 5.9$	1.6	$< 3.3$
$K^0\bar{K}^0$	$2.0 \pm 1.9$	1.3	$< 1.5$

TABLE III: Uncertainties on the reconstruction efficiencies ( $\delta\epsilon$ ) along with the test samples that are used.

Source	$\delta\epsilon/\epsilon [\%]$	Test sample
track finding	1.0	$D^{*+} \rightarrow D^0(\rightarrow K_S^0\pi^+\pi^-)\pi^+$
$K_S^0$	4.4	$D^+ \rightarrow K_S^0\pi^+, K^-\pi^+\pi^+$
$\pi^0$	3.5	$\eta \rightarrow \pi^0\pi^0\pi^0, \gamma\gamma$
$\mathcal{R}_K$	0.2	$D^{*+} \rightarrow D^0(\rightarrow K^-\pi^+)\pi^+$
$\mathcal{R}_s$	1.3–7.8	$B^+ \rightarrow \bar{D}^0(\rightarrow K^+\pi^-, K^+\pi^-\pi^0)\pi^+$

TABLE IV: Partial width ratios of  $B \rightarrow K\pi$  and  $\pi\pi$  decays. The errors are quoted in the same manner as in Table II.

Modes	Ratio
$\Gamma(K^+\pi^-) / \Gamma(K^0\pi^+)$	$0.91 \pm 0.09 \pm 0.06$
$\Gamma(K^+\pi^-) / 2\Gamma(K^0\pi^0)$	$0.79 \pm 0.16 \pm 0.09$
$2\Gamma(K^+\pi^0) / \Gamma(K^0\pi^+)$	$1.09 \pm 0.15 \pm^{+0.13}_{-0.10}$
$\Gamma(\pi^+\pi^-) / \Gamma(K^+\pi^-)$	$0.24 \pm 0.03 \pm 0.02$
$\Gamma(\pi^+\pi^0) / \Gamma(K^0\pi^0)$	$0.39 \pm 0.12 \pm 0.06$
$2\Gamma(\pi^+\pi^0) / \Gamma(K^0\pi^+)$	$0.45 \pm 0.12 \pm 0.05$
$2\Gamma(\pi^+\pi^0) / \Gamma(\pi^+\pi^-)$	$2.10 \pm 0.58 \pm 0.25$
$\Gamma(\pi^0\pi^0) / \Gamma(\pi^+\pi^-)$	$0.39 \pm 0.15 \pm 0.05$
$\Gamma(\pi^0\pi^0) / \Gamma(\pi^+\pi^0)$	$0.37 \pm 0.16 \pm 0.05$

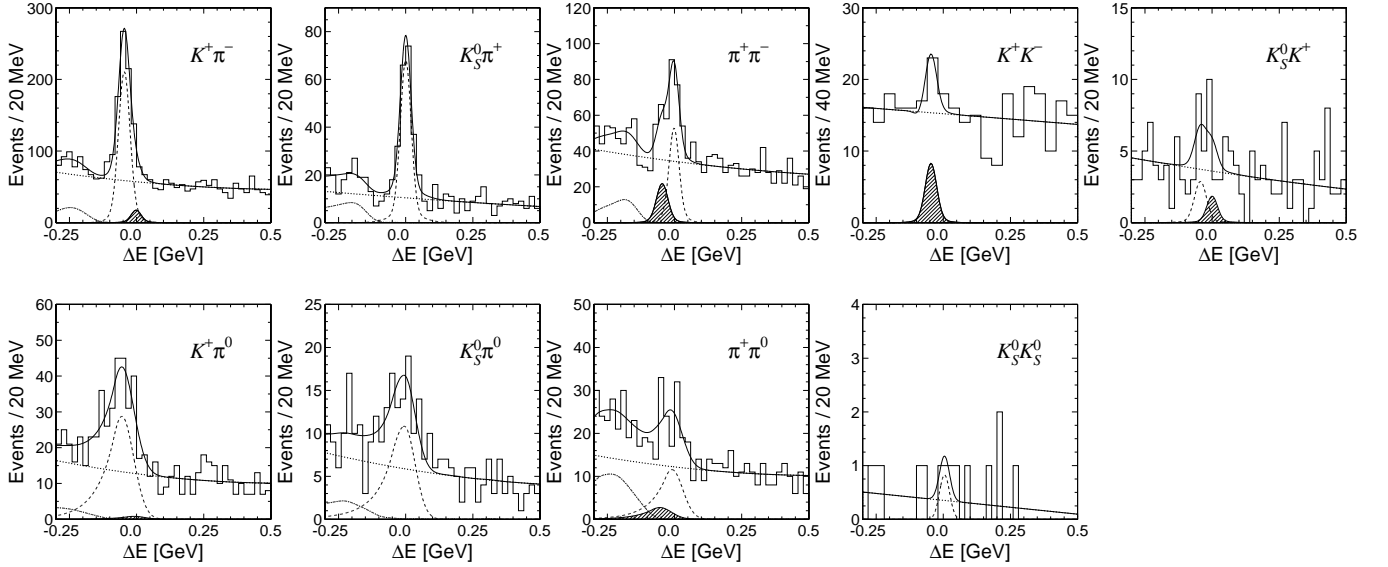


FIG. 1:  $\Delta E$  distributions for  $B \rightarrow K\pi$ ,  $\pi^+\pi^-$ ,  $\pi^+\pi^0$  and  $K\bar{K}$  decays. Fit results are shown as the solid, dashed, dotted and dot-dashed curves for the total, signal,  $q\bar{q}$  background and the other charmless  $B$  decays, respectively. In addition, reflections due to  $K^\pm/\pi^\pm$  misidentification are shown as hatched areas.